Implications of reciprocity for the spectra of equilibrium and nonequilibrium Casimir forces

Hideo Iizuka [1,*] and Shanhui Fan [2,†]

[1]*Toyota Central R&D Labs., Inc., Nagakute, Aichi 480 1192, Japan*

[2]*Department of Electrical Engineering, Ginzton Laboratory, Stanford University, Stanford, California 94305, USA*

(Received 27 June 2023; revised 12 August 2023; accepted 14 August 2023; published 24 August 2023)

We investigate the Casimir forces in a planar two-body system with each backed by a plate of perfect electric conductor. We show that for the equilibrium Casimir forces, the spectra of the Casmir pressure are symmetric in the wave-vector space for reciprocal systems, and become asymmetric when reciprocity is broken. Therefore, there is a distinct signature of reciprocity in the spectra of equilibrium Casimir forces. The same signature also holds for the lateral force, which is nonzero only in the nonequilibrium case. On the other hand, for the pressure in the nonequilibrium scenario, such an asymmetry can arise for both reciprocal and nonreciprocal cases. We also elucidate a relation on the Casmir force that is connected to Newton's third law. We show that Newton's third law holds for every frequency and wave vector, as long as no exchange of photons occurs between the two-body system and the environment. Newton's third law is distinct from the reciprocity constraints. We illustrate the theoretical results with numerical calculations described by anisotropic permittivity tensors that are either symmetric and hence reciprocal, or asymmetric and hence nonreciprocal.

DOI: 10.1103/PhysRevB.108.075429

I. INTRODUCTION

There is a large body of literature on Casimir forces in equilibrium [1–10] and nonequilibrium [11–18], exploring various materials [19–24] and geometries [25–28], and finding opportunities in applications towards nanoscale mechanical systems [29–32]. Most existing works on Casimir forces use reciprocal material systems that satisfy the Lorentz reciprocity. The Lorentz reciprocity implies a certain symmetry in Green's function of a system and is applicable when the permittivity and permeability of the materials are scalar or symmetric tensors [33]. On the other hand, by introducing nonreciprocal materials, e.g., heavily doped semiconductors under external magnetic field or magnetic Weyl semimetals, one can achieve unusual effects in Casimir forces such as repulsive pressures [34–41], lateral forces [42–46], and torques [47–49]. In spite of these recent developments, however, there has not been a study of the implications of reciprocity on the spectra of Casimir forces.

The effects of Casimir forces are closely related to the effects of near-field heat transfer since both effects arise from electromagnetic fluctuations. Recently, the implications of reciprocity on the spectra of near-field heat transfer have been considered in Ref. [50]. As a step further, in this paper, we consider the role of reciprocity in the spectra of Casimir forces in a planar two-body system. Understanding of the symmetry properties of these spectra is of importance for the control of the Casimir forces. The spectra of the Casimir forces are physical quantities. Therefore, they in principle can be measured, even though there has not been any direct measurement of such spectra.

Casimir forces can occur in both equilibrium and nonequilibrium systems. In equilibrium systems, all bodies and the environment have the same temperature T, which can be either at 0 K or at a nonzero value. These equilibrium systems can only exhibit Casimir pressures. We show that the spectra of the Casmir pressure are symmetric in the wave-vector space (k space) for reciprocal systems, and can become asymmetric when reciprocity is broken. Therefore, there is a distinct signature of reciprocity in the spectra of equilibrium Casimir forces. In nonequilibrium systems, the bodies and the environment may have different temperatures. These systems can exhibit both the pressure and the lateral force. The spectra of the lateral force are symmetric in the k space for the reciprocal system, and can become asymmetric when the reciprocity is broken. On the other hand, the spectra of the pressure in the nonequilibrium systems can exhibit asymmetry for both reciprocal and nonreciprocal cases. For both equilibrium and nonequilibrium systems, we also elucidate a relation on the Casmir force that is connected to Newton's third law. We show that Newton's third law holds for every frequency and wave vector, as long as no exchange of photons occurs between the two-body system and the environment. Thus, while Newton's third law has a form that is somewhat similar to some of the constraints associated with reciprocity, it is in fact distinct from the reciprocity constraints. We illustrate the theoretical results with numerical calculations described by anisotropic permittivity tensors that are either symmetric and hence reciprocal, or asymmetric and hence nonreciprocal.

The rest of the paper is organized as follows. In Sec. II, we present a model system consisting of two planar bodies for the investigation of the Casimir pressure and lateral force. In Sec. III, we present the formalism of the Casimir pressure,

*hiizuka@mosk.tytlabs.co.jp

†shanhui@stanford.edu

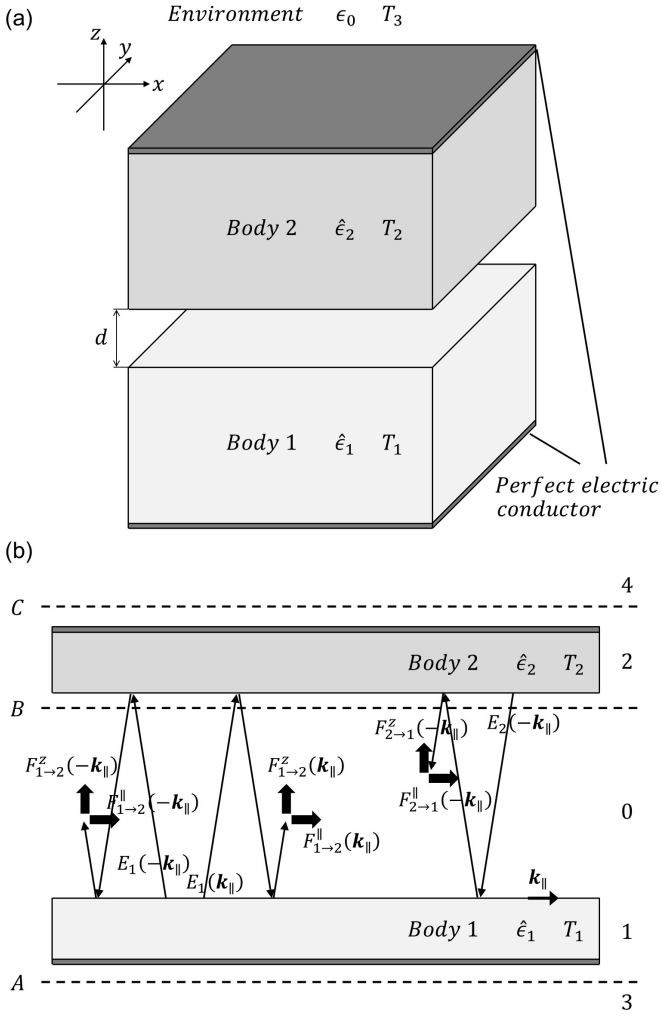

FIG. 1. (a) Geometry of a system consisting of two planar bodies with each backed by plate of perfect electric conductor. (b) Schematic illustration of Casimir pressures and lateral forces for in-plane wave vectors $+\boldsymbol{k}_\parallel$ and $-\boldsymbol{k}_\parallel$ at angle φ. Dashed lines labeled by A, B, and C denote boundaries below body 1, between body 1 and body 2, and above body 2.

and analytically and numerically verify the implication of symmetry for reciprocal systems in the equilibrium Casimir pressure. In addition, we elucidate a relation on the Casimir pressure that is connected to Newton's third law. In Sec. IV, we present an investigation of the lateral Casimir forces. This paper is then concluded in Sec. V.

II. MODEL SYSTEM

We consider a system consisting of two planar bodies with each backed by a plate of perfect electric conductor, as shown in Fig. 1(a). The bodies are maintained at temperatures T_1 and T_2, respectively, and are separated by the vacuum gap size d. We assume that the bodies are much thicker than the dominant wavelength that contributes to the Casimir forces, and the regions outside the two plates of perfect electric conductor consist of semi-infinite vacuum with temperature T_3. This system is in equilibrium if and only if $T_1 = T_2 = T_3$, and is in nonequilibrium if at least one of the three temperatures is different. In this paper we mostly concentrate on the case where $T_1 \neq T_2$ when we consider nonequilibrium systems.

We use a coordinate system as indicated in Fig. 1(a). We refer to the electromagnetic force along the z axis as the Casimir pressure or the pressure, and the electromagnetic force in the xy plane as the lateral Casimir force or the lateral force. Figure 1(b) shows the schematic illustration of the Casimir pressures and lateral forces arising from body 1 and from body 2. These forces are evaluated by integration of Maxwell's stress tensor in the boundaries as indicated in Fig. 1(b). We will present the derivation of the formalism for the forces acting on body 2, and discuss symmetry of the spectra with respect to the in-plane wave vector $\boldsymbol{k}_\parallel$.

We assume that body 1 consists of a heavily doped semiconductor with its permittivity being a 3×3 diagonal permittivity tensor $\hat{\epsilon}_1 = \epsilon_p \hat{I}$, where $\hat{I}$ is a 3×3 identity matrix and $\epsilon_p = 1 - \frac{\omega_p^2}{\omega(\omega + i\Gamma)}$ as determined by the Drude model, with ω_p and Γ being the plasma frequency and the damping rate, respectively. We select $\Gamma = 0.1\omega_p$ for numerical calculations. For the nonreciprocal case, we consider body 2 consisting of the same heavily doped semiconductor as body 1, but subject to a magnetic field B along the y direction. Such a material is described by a 3×3 permittivity tensor $\hat{\epsilon}_2 = \hat{\epsilon}_2^A$, where [50] where

$$\hat{\epsilon}_2^A = \begin{pmatrix} \epsilon_d & 0 & i\epsilon_f \\ 0 & \epsilon_p & 0 \\ -i\epsilon_f & 0 & \epsilon_d \end{pmatrix}, \tag{1}$$

$\epsilon_d = 1 - \frac{\omega_p^2(1+i\frac{\Gamma}{\omega})}{(\omega+i\Gamma)^2-\omega_c^2}$ and $\epsilon_f = -\frac{\omega_p^2 \frac{\omega_c}{\omega}}{(\omega+i\Gamma)^2-\omega_c^2}$. $\omega_c = \frac{eB}{m}$ is the cyclotron frequency, with e and m being the electron charge and the electron mass, respectively. The hat denotes matrix. We note that $\hat{\epsilon}_2^A$ is asymmetric, indicating that the reciprocity is broken in this system. We choose $\omega_c = 0.2\omega_p$ for numerical calculations. To illustrate the effect of reciprocity breaking, we also consider a reciprocal case where body 2 instead has a permittivity $\hat{\epsilon}_2 = \hat{\epsilon}_2^S$, where

$$\hat{\epsilon}_2^S = \begin{pmatrix} \epsilon_d & 0 & \epsilon_f \\ 0 & \epsilon_p & 0 \\ \epsilon_f & 0 & \epsilon_d \end{pmatrix}, \tag{2}$$

has a very similar form as $\hat{\epsilon}_2^A$, but it is symmetric. Both $\hat{\epsilon}_2^A$ and $\hat{\epsilon}_2^S$ have the same mirror-symmetry property. Both are mirror symmetric with respect to the zx plane. Both are not mirror symmetric with respect to any plane parallel to the z axis except for the zx plane. Throughout the paper we choose the spacing between the bodies $d = \lambda_p/20$, where $\lambda_p = 2\pi c/\omega_p$ and c is the speed of light.

The dispersion equation for the surface modes of the system of Fig. 1(a) is given by

$$\left(\frac{\frac{\epsilon_d^2 - \epsilon_f^2}{\epsilon_d}\cos^2(\varphi) + \epsilon_p \sin^2(\varphi)}{\kappa_{z2}} + \frac{1}{\kappa_{z0}} - i^w \frac{\frac{\epsilon_f}{\epsilon_d} k_\parallel \cos(\varphi)}{\kappa_{z0}\kappa_{z2}} \right)$$
$$\times \left(\frac{\epsilon_p}{\kappa_{z1}} + \frac{1}{\kappa_{z0}} \right) e^{\kappa_{z0} d} - \left(\frac{\frac{\epsilon_d^2 - \epsilon_f^2}{\epsilon_d}\cos^2(\varphi) + \epsilon_p \sin^2(\varphi)}{\kappa_{z2}} - \frac{1}{\kappa_{z0}} \right.$$
$$\left. + i^w \frac{\frac{\epsilon_f}{\epsilon_d} k_\parallel \cos(\varphi)}{\kappa_{z0}\kappa_{z2}} \right) \left(\frac{\epsilon_p}{\kappa_{z1}} - \frac{1}{\kappa_{z0}} \right) e^{-\kappa_{z0} d} = 0, \tag{3}$$

where $w = 1$ for the reciprocal material [Eq. (2)] and $w = 2$ for the nonreciprocal material [Eq. (1)]. Here, φ is the angle from the x axis to the in-plane wave vector. The wave-vector components normal to the surfaces of the bodies are $\kappa_{z0} = \sqrt{k_\parallel^2 - k_0^2}$ ($k_0 < k_\parallel$, where k_0 is the free-space wave number and $k_\parallel = |\boldsymbol{k}_\parallel|$ is the magnitude of the in-plane wave vector) for the region of the vacuum gap and $\kappa_{z1} = \sqrt{k_\parallel^2 - \epsilon_p k_0^2}$ for the region of body 1. For a given ω and $\boldsymbol{k}_\parallel$, κ_{z2} for the region of body 2 is obtained by solving the equation $\nabla \times \nabla \times \boldsymbol{E} - \omega^2 \mu_0 \epsilon_0 \hat{\epsilon}_2 \boldsymbol{E} = 0$. The detailed derivation of Eq. (3) is found in Appendix A.

III. CASIMIR PRESSURE

In this section we consider the implications of reciprocity on the spectrum of the Casmir pressure for the system shown in Fig. 1(a). In Sec. III A, we derive the formalism of the Casimir pressure in the system of Fig. 1(a). In Sec. III B, we discuss the symmetry property of the pressure in the wave-vector space, based on the analytic formalism derived in Sec. III A. In Sec. III C, we elucidate a relation on the pressure that is connected to Newton's third law and discuss the difference between reciprocity constraints and Newton's third law. In Sec. III D, the symmetry argument is numerically verified.

A. Formalism of the Casimir pressure

We define the Casimir pressure $F^z_{1\to2}(\boldsymbol{r}_\parallel, z, t, T_1)$ from body 1 to body 2 as the electromagnetic pressure exerted on body 2 due to the fluctuating current sources in body 1. This pressure is computed from the electric field $\boldsymbol{E}(\boldsymbol{r}_\parallel, z, t, T_1)$ and the magnetic field $\boldsymbol{H}(\boldsymbol{r}_\parallel, z, t, T_1)$ in the vacuum gap, where $\boldsymbol{r}_\parallel$ is the in-plane real-space vector. The pressure has the form

$$F^z_{1\to2}(\boldsymbol{r}_\parallel, z, t, T_1) = \left\langle \tfrac{1}{2}\epsilon_0 \left(E_z^2 - E_\parallel^2\right) + \tfrac{1}{2}\mu_0 \left(H_z^2 - H_\parallel^2\right)\right\rangle, \quad (4)$$

where μ_0 is the free-space permeability. Here, t is time. In the right-hand side of Eq. (4), $(\boldsymbol{r}_\parallel, z, t, T_1)$ is suppressed, and the ensemble average, denoted by a pair of angle brackets, has been used. We use the Fourier transformation convention in time and space as

$$A(t) = \mathrm{Re}\int_0^\infty d\omega A(\omega) e^{-i\omega t}, \quad (5)$$

$$A(\boldsymbol{r}_\parallel) = \int_{-\infty}^{\infty} \frac{d\boldsymbol{k}_\parallel}{(2\pi)^2} A(\boldsymbol{k}_\parallel) e^{i\boldsymbol{k}_\parallel \cdot \boldsymbol{r}_\parallel}. \quad (6)$$

$F^z_{1\to2}(\boldsymbol{r}_\parallel, z, t, T_1)$ is independent of $\boldsymbol{r}_\parallel$, z, and t due to translational symmetry, the absence of absorption in the vacuum gap, and the fact that the underlying quantum and thermal fluctuations are stationary random processes, respectively. Also, we have

$$\begin{aligned}&\langle \boldsymbol{E}(\omega, \boldsymbol{k}_\parallel, z, T_1) \boldsymbol{E}^\dagger(\omega', \boldsymbol{k}_\parallel', z, T_1)\rangle \\ &\quad = \langle \boldsymbol{E}(\omega, \boldsymbol{k}_\parallel, z, T_1) \boldsymbol{E}^\dagger(\omega, \boldsymbol{k}_\parallel, z, T_1)\rangle \delta(\omega - \omega') \delta(\boldsymbol{k}_\parallel - \boldsymbol{k}_\parallel').\end{aligned} \quad (7)$$

From Eqs. (4)–(7), we have

$$F^z_{1\to2} = \int_0^\infty d\omega \int_{-\infty}^{\infty} \frac{d\boldsymbol{k}_\parallel}{(2\pi)^4} T^z_{1\to2}(\omega, \boldsymbol{k}_\parallel, T_1), \quad (8)$$

where

$$T^z_{1\to2}(\omega, \boldsymbol{k}_\parallel, T_1) = \tfrac{1}{4}\langle \epsilon_0 (|E_z|^2 - |E_\parallel|^2) + \mu_0 (|H_z|^2 - |H_\parallel|^2)\rangle. \quad (9)$$

$(\omega, \boldsymbol{k}_\parallel, T_1)$ is suppressed for the electric- and magnetic-field components in the right-hand side of Eq. (9). Below, in our formalism, $(\omega, \boldsymbol{k}_\parallel, T_1)$, $(\omega, \boldsymbol{k}_\parallel)$, or (ω) is suppressed.

In the calculations of the Casmir pressure, the electromagnetic properties of the bodies enter in terms of their reflection matrices. The reflection matrix at the surface of body l for light incident from the vacuum has the form

$$\hat{R}_l = \begin{pmatrix} R_l^{ss} & R_l^{ps} \\ R_l^{sp} & R_l^{pp} \end{pmatrix}, \quad (10)$$

where $R_l^{\alpha\beta}$ is the reflection coefficient from the α-polarized incident wave to the β-polarized reflected wave. For s polarization (p polarization), the electric (magnetic) field is normal to the plane spanned by the wave vector $\boldsymbol{k}$ and the z axis. Each component of the reflection matrix in Eq. (10) is obtained based on the convention of $\boldsymbol{s} \times \boldsymbol{p} = \boldsymbol{k}/|\boldsymbol{k}|$, with $\boldsymbol{s}$ and $\boldsymbol{p}$ being the unit vectors for the s-polarized and p-polarized electric fields. In the absence of body 2, we assume the field emitted by body 1 to be $\boldsymbol{E}_1$. When body 2 is present, in the vacuum gap, there are multiple reflections of the electromagnetic wave that is emitted from body 1. As a result of such multiple reflections, near the surface of body 2, the field due to the emission from body 1 is expressed as

$$\begin{aligned}\boldsymbol{E} &= e^{ik_{z0}d}(\boldsymbol{E}_1 + \hat{R}_1\hat{R}_2 e^{i2k_{z0}d}\boldsymbol{E}_1 + \hat{R}_1\hat{R}_2\hat{R}_1\hat{R}_2 e^{i4k_{z0}d}\boldsymbol{E}_1 + \cdots) \\ &= e^{ik_{z0}d}\hat{D}_{12}\boldsymbol{E}_1,\end{aligned} \quad (11)$$

where $\hat{D}_{12} = (\hat{I} - \hat{R}_1\hat{R}_2 e^{i2k_{z0}d})^{-1}$. $k_{z0} = \sqrt{k_0^2 - k_\parallel^2}$ $(k_0 > k_\parallel)$, $[k_{z0} = i\kappa_{z0}$ $(k_0 < k_\parallel)]$ is the wave-vector component normal to the surfaces of the bodies for propagation waves (evanescent waves). Substituting the electric field of Eq. (11) and the corresponding magnetic field into Eq. (9), we have the forms of contributions to the pressure from propagation and evanescent waves, respectively, as

$$\begin{aligned}&T^z_{1\to2}(\omega, \boldsymbol{k}_\parallel, T_1) \\ &= \begin{cases} \mathrm{Tr}\left[-\frac{k_{z0}}{2Z\omega}(\hat{I} + \hat{R}_2^\dagger\hat{R}_2)\hat{D}_{12}\langle \boldsymbol{E}_1\boldsymbol{E}_1^\dagger\rangle \hat{D}_{12}^\dagger\right], & (k_\parallel < k_0) \\ \mathrm{Tr}\left[-\frac{i\kappa_{z0}}{2Z\omega}(\hat{R}_2^\dagger + \hat{R}_2)\hat{D}_{12}\langle \boldsymbol{E}_1\boldsymbol{E}_1^\dagger\rangle \hat{D}_{12}^\dagger e^{-2\kappa_{z0}d}\right], & (k_\parallel > k_0) \end{cases},\end{aligned} \quad (12)$$

where $Z = \frac{k_0}{k_{z0}}\sqrt{\frac{\mu_0}{\epsilon_0}}$, $(k_\parallel < k_0)$ $[Z = \frac{k_0}{i\kappa_{z0}}\sqrt{\frac{\mu_0}{\epsilon_0}}, (k_\parallel > k_0)]$ is the impedance of vacuum for propagation waves (evanescent waves). $\langle \boldsymbol{E}_1\boldsymbol{E}_1^\dagger\rangle$ is the correlation of the electric field emitted from body 1 near the surface of body 1 and is given by [50]

$$\begin{aligned}&\langle \boldsymbol{E}_1\boldsymbol{E}_1^\dagger\rangle \\ &= \begin{cases} (2\pi)^2 \frac{Z\hbar\omega}{\pi}\left[n(\omega, T_1) + \frac{1}{2}\right](\hat{I} - \hat{R}_1\hat{R}_1^\dagger), & (k_\parallel < k_0) \\ (2\pi)^2 \frac{Z\hbar\omega}{\pi}\left[n(\omega, T_1) + \frac{1}{2}\right](\hat{R}_1 - \hat{R}_1^\dagger), & (k_\parallel > k_0) \end{cases},\end{aligned} \quad (13)$$

where $n(\omega, T) = (e^{(\hbar\omega/k_BT)} - 1)^{-1}$ is the number of thermal photons in a single optical mode at frequency ω and temperature T, with $\hbar$ and k_B being the reduced Planck constant and

Boltzmann constant, respectively. From Eqs. (8), (12), and (13), we have the pressure from body 1 to body 2:

$$F^z_{1\to2}(\omega,\boldsymbol{k}_\parallel,T_1)=\left[n(\omega,T_1)+\frac{1}{2}\right]\frac{\hbar|k_{z0}|}{8\pi^3}\tilde{F}^z_{1\to2}(\omega,\boldsymbol{k}_\parallel), \quad (14)$$

where the exchange function

$$\tilde{F}^z_{l\to m}(\omega,\boldsymbol{k}_\parallel) = \begin{cases} \mathrm{Tr}[-(\hat{I}+\hat{R}^\dagger_m\hat{R}_m)\hat{D}_{lm}(\hat{I}-\hat{R}_l\hat{R}^\dagger_l)\hat{D}^\dagger_{lm}], & (k_\parallel<k_0) \\ \mathrm{Tr}[-i(\hat{R}^\dagger_m+\hat{R}_m)\hat{D}_{lm}(\hat{R}_l-\hat{R}^\dagger_l)\hat{D}^\dagger_{lm}e^{-2\kappa_{z0}d}], & (k_\parallel>k_0) \end{cases} \quad (15)$$

$(l,m)=(1,2),(2,1)$. We note that the treatment above is applicable for both reciprocal and nonreciprocal materials, and the symmetry properties of the spectra of the Casimir pressure can be determined by analyzing $\tilde{F}^z_{l\to m}$ as defined in Eq. (15). The pressure from body 2 to body 1 can be determined by exchanging the subscripts 1 and 2 in Eq. (14).

The total pressure acting on each of bodies 1 and 2 has contributions from the sources in body 1, body 2, and vacuum. By combining the contributions from all three sources, the total pressures acting on bodies 1 and 2 are given by

$$F^z_{1,2}(T_1,T_2,T_3)=\int_0^\infty d\omega\int_{-\infty}^\infty d\boldsymbol{k}_\parallel F^z_{1,2}(\omega,\boldsymbol{k}_\parallel,T_1,T_2,T_3), \quad (16)$$

where

$$F^z_1(\omega,\boldsymbol{k}_\parallel,T_1,T_2,T_3)=F^z_{1\to2}(\omega,\boldsymbol{k}_\parallel,T_1)+F^z_{2\to1}(\omega,\boldsymbol{k}_\parallel,T_2)+F^z_{ext,1}(\omega,\boldsymbol{k}_\parallel,T_3), \quad (17)$$

$$F^z_2(\omega,\boldsymbol{k}_\parallel,T_1,T_2,T_3)=-F^z_{1\to2}(\omega,\boldsymbol{k}_\parallel,T_1)-F^z_{2\to1}(\omega,\boldsymbol{k}_\parallel,T_2)+F^z_{ext,2}(\omega,\boldsymbol{k}_\parallel,T_3), \quad (18)$$

with

$$F^z_{\mathrm{ext},2}(\omega,\boldsymbol{k}_\parallel,T_3)=-F^z_{\mathrm{ext},1}(\omega,\boldsymbol{k}_\parallel,T_3) =-\left[n(\omega,T_3)+\frac{1}{2}\right]\frac{\hbar k_{z0}}{2\pi^3}, \quad (19)$$

where we have used $\tilde{F}^z_{\mathrm{ext},2}=-\tilde{F}^z_{\mathrm{ext},1}=\mathrm{Tr}[-2\hat{I}]=-4$. In Eq. (16), $F^z_1>0$ indicates an attractive force on body 1, whereas $F^z_2>0$ indicates a repulsive force on body 2. In deriving Eqs. (17) and (18), we have used the relation

$$F^z_{1\to1}(\omega,\boldsymbol{k}_\parallel,T_1)=-F^z_{1\to2}(\omega,\boldsymbol{k}_\parallel,T_1), \quad (20)$$

$$F^z_{2\to2}(\omega,\boldsymbol{k}_\parallel,T_2)=-F^z_{2\to1}(\omega,\boldsymbol{k}_\parallel,T_2). \quad (21)$$

Both terms in each of Eqs. (20) and (21) in fact result from the integration of the stress tensor on the same boundary B from the same source, i.e., body 1 for Eq. (20) and body 2 for Eq. (21). The sign difference arises since the normal directions required for the two integrations are opposite to each other. The first and the second terms in Eqs. (17) and (18) correspond to the force components at the boundary in the vacuum gap [boundary B in Fig. 1(b)], arising from bodies 1 and 2, respectively. The third term in Eq. (17) corresponds to the force component at the exterior boundary of body 1 [boundary A in Fig. 1(b)], arising from the vacuum environment in the $-z$ region. Similarly, the third term in Eq. (18) corresponds to the force component at the exterior boundary of body 2 [boundary C in Fig. 1(b)], arising from the vacuum environment in the $+z$ region. The result in Eq. (19) arises due to the perfect electric conductor plates at the exterior surfaces of bodies 1 and 2.

B. Symmetry properties for the Casimir pressure

Using the formalism as developed in the previous section, in this section we discuss the symmetry properties of the spectrum of Casmir pressure in the $\boldsymbol{k}_\parallel$ space. We focus on the relation between the Casimir pressure at $\boldsymbol{k}_\parallel$ and at $-\boldsymbol{k}_\parallel$. This is motivated by Ref. [50], which has shown that the relation between the heat-transfer coefficient at $\boldsymbol{k}_\parallel$ and $-\boldsymbol{k}_\parallel$ is a constraint by reciprocity. Here, we show that a similar reciprocity constraint is present for the Casimir pressure as well.

As the first main result of the paper, we show for a reciprocal system, in equilibrium with $T_1=T_2=T_3=T$, the spectra of the pressure acting on each of bodies 1 and 2 are symmetric in the $\boldsymbol{k}_\parallel$ space:

$$F^z_{1,2}(\omega,\boldsymbol{k}_\parallel,T,T,T)=F^z_{1,2}(\omega,-\boldsymbol{k}_\parallel,T,T,T). \quad (22)$$

We prove Eq. (22) from Eqs. (17) and (18). Since the third term in Eqs. (17) and (18) is constant in the ω–$\boldsymbol{k}_\parallel$ space, we focus on the first two terms. The reflection matrix for each of the bodies in the reciprocal system satisfies [51]

$$\hat{R}_l(-\boldsymbol{k}_\parallel)=\hat{\sigma}_z\hat{R}^T_l(\boldsymbol{k}_\parallel)\hat{\sigma}_z, \quad (23)$$

where $\hat{\sigma}_z=\mathrm{diag}(1,-1)$. From Eq. (15), we have

$$\tilde{F}^z_{1\to2}(-\boldsymbol{k}_\parallel) = \begin{cases} \mathrm{Tr}[-(\hat{I}+\hat{R}^\dagger_2(-\boldsymbol{k}_\parallel)\hat{R}_2(-\boldsymbol{k}_\parallel))\hat{D}_{12}(-\boldsymbol{k}_\parallel)(\hat{I}-\hat{R}_1(-\boldsymbol{k}_\parallel)\hat{R}^\dagger_1(-\boldsymbol{k}_\parallel))\hat{D}^\dagger_{12}(-\boldsymbol{k}_\parallel)], & (k_\parallel<k_0) \\ \mathrm{Tr}[-i(\hat{R}^\dagger_2(-\boldsymbol{k}_\parallel)+\hat{R}_2(-\boldsymbol{k}_\parallel))\hat{D}_{12}(-\boldsymbol{k}_\parallel)(\hat{R}_1(-\boldsymbol{k}_\parallel)-\hat{R}^\dagger_1(-\boldsymbol{k}_\parallel))\hat{D}^\dagger_{12}(-\boldsymbol{k}_\parallel)e^{-2\kappa_{z0}d}]. & (k_\parallel>k_0) \end{cases} \quad (24)$$

Using Eq. (23) and the corresponding relation $\hat{D}_{21}(-\boldsymbol{k}_\parallel)=\hat{\sigma}_z\hat{D}^T_{12}(\boldsymbol{k}_\parallel)\hat{\sigma}_z$, Eq. (24) is rewritten as

$$\tilde{F}^z_{1\to2}(-\boldsymbol{k}_\parallel) = \begin{cases} \mathrm{Tr}[-(\hat{I}-\hat{R}^\dagger_1(\boldsymbol{k}_\parallel)\hat{R}_1(\boldsymbol{k}_\parallel))\hat{D}_{21}(\boldsymbol{k}_\parallel)(\hat{I}+\hat{R}_2(\boldsymbol{k}_\parallel)\hat{R}^\dagger_2(\boldsymbol{k}_\parallel))\hat{D}^\dagger_{21}(\boldsymbol{k}_\parallel)], & (k_\parallel<k_0) \\ \mathrm{Tr}[i(\hat{R}^\dagger_1(\boldsymbol{k}_\parallel)-\hat{R}_1(\boldsymbol{k}_\parallel))\hat{D}_{21}(\boldsymbol{k}_\parallel)(\hat{R}_2(\boldsymbol{k}_\parallel)+\hat{R}^\dagger_2(\boldsymbol{k}_\parallel))\hat{D}^\dagger_{21}(\boldsymbol{k}_\parallel)e^{-2\kappa_{z0}d}]. & (k_\parallel>k_0) \end{cases} \quad (25)$$

Comparing Eq. (25) with Eq. (15), $\tilde{F}^z_{1\to2}(\boldsymbol{k}_\parallel)$ and $\tilde{F}^z_{1\to2}(-\boldsymbol{k}_\parallel)$ may not be equal for the reciprocal system [52]. Similarly, one can check that $\tilde{F}^z_{2\to1}(\boldsymbol{k}_\parallel)$ and $\tilde{F}^z_{2\to1}(-\boldsymbol{k}_\parallel)$ may not be equal for the reciprocal system. On the other hand,

$$\tilde{F}^z_{1\to2}(-\boldsymbol{k}_\parallel)+\tilde{F}^z_{2\to1}(-\boldsymbol{k}_\parallel)=\begin{cases}\mathrm{Re\ Tr}[-2\hat{I}-2(\hat{R}_1(-\boldsymbol{k}_\parallel)\hat{D}_{21}(-\boldsymbol{k}_\parallel)\hat{R}_2(-\boldsymbol{k}_\parallel)+\hat{R}_2(-\boldsymbol{k}_\parallel)\hat{D}_{12}(-\boldsymbol{k}_\parallel)\hat{R}_1(-\boldsymbol{k}_\parallel))e^{i2k_{z0}d}], & (k_\parallel<k_0)\\ \mathrm{Im\ Tr}[2\hat{R}_1(-\boldsymbol{k}_\parallel)\hat{D}_{21}(-\boldsymbol{k}_\parallel)\hat{R}_2(-\boldsymbol{k}_\parallel)+2\hat{R}_2(-\boldsymbol{k}_\parallel)\hat{D}_{12}(-\boldsymbol{k}_\parallel)\hat{R}_1(-\boldsymbol{k}_\parallel)]e^{-2\kappa_{z0}d}. & (k_\parallel>k_0)\end{cases} \tag{26}$$

Substituting Eq. (23) into Eq. (26), we have

$$\tilde{F}^z_{1\to2}(-\boldsymbol{k}_\parallel)+\tilde{F}^z_{2\to1}(-\boldsymbol{k}_\parallel)=\begin{cases}\mathrm{Re\ Tr}[-2\hat{I}-2(\hat{R}_1(\boldsymbol{k}_\parallel)\hat{D}_{21}(\boldsymbol{k}_\parallel)\hat{R}_2(\boldsymbol{k}_\parallel)+\hat{R}_2(\boldsymbol{k}_\parallel)\hat{D}_{12}(\boldsymbol{k}_\parallel)\hat{R}_1(\boldsymbol{k}_\parallel))e^{i2k_{z0}d}], & (k_\parallel<k_0)\\ \mathrm{Im\ Tr}[2\hat{R}_1(\boldsymbol{k}_\parallel)\hat{D}_{21}(\boldsymbol{k}_\parallel)\hat{R}_2(\boldsymbol{k}_\parallel)+2\hat{R}_2(\boldsymbol{k}_\parallel)\hat{D}_{12}(\boldsymbol{k}_\parallel)\hat{R}_1(\boldsymbol{k}_\parallel)]e^{-2\kappa_{z0}d}. & (k_\parallel>k_0)\end{cases} \tag{27}$$

Therefore, for the reciprocal system, the summation of the exchange functions is symmetric:

$$\tilde{F}^z_{1\to2}(\omega,\boldsymbol{k}_\parallel)+\tilde{F}^z_{2\to1}(\omega,\boldsymbol{k}_\parallel)=\tilde{F}^z_{1\to2}(\omega,-\boldsymbol{k}_\parallel)+\tilde{F}^z_{2\to1}(\omega,-\boldsymbol{k}_\parallel), \tag{28}$$

which proves Eq. (22).

The discussion above is for the equilibrium case where $T_1=T_2$. For the nonequilibrium case with $T_1\neq T_2$, it is no longer sufficient to discuss the symmetry properties of the pressure by considering the exchange function only. Instead, from Eqs. (14), (17), and (18), we have

$$\begin{aligned}&F^z_1(\omega,\boldsymbol{k}_\parallel,T_1,T_2,T_3)\\&=\left[n(\omega,T_1)+\frac{1}{2}\right]\frac{\hbar|k_{z0}|}{8\pi^3}\tilde{F}^z_{1\to2}(\omega,\boldsymbol{k}_\parallel)\\&\quad+\left[n(\omega,T_2)+\frac{1}{2}\right]\frac{\hbar|k_{z0}|}{8\pi^3}\tilde{F}^z_{2\to1}(\omega,\boldsymbol{k}_\parallel)\\&\quad+\left[n(\omega,T_3)+\frac{1}{2}\right]\frac{\hbar k_{z0}}{8\pi^3}\tilde{F}^z_{\mathrm{ext},1}(\omega,\boldsymbol{k}_\parallel),\end{aligned} \tag{29}$$

and

$$\begin{aligned}&F^z_2(\omega,\boldsymbol{k}_\parallel,T_1,T_2,T_3)\\&=-\left[n(\omega,T_1)+\frac{1}{2}\right]\frac{\hbar|k_{z0}|}{8\pi^3}\tilde{F}^z_{1\to2}(\omega,\boldsymbol{k}_\parallel)\\&\quad-\left[n(\omega,T_2)+\frac{1}{2}\right]\frac{\hbar|k_{z0}|}{8\pi^3}\tilde{F}^z_{2\to1}(\omega,\boldsymbol{k}_\parallel)\\&\quad+\left[n(\omega,T_3)+\frac{1}{2}\right]\frac{\hbar k_{z0}}{8\pi^3}\tilde{F}^z_{\mathrm{ext},2}(\omega,\boldsymbol{k}_\parallel).\end{aligned} \tag{30}$$

From Eqs. (29) and (30), we can show mathematically that when $T_1\neq T_2$, $F^z_{1,2}(\omega,\boldsymbol{k}_\parallel,T_1,T_2,T_3)\neq F^z_{1,2}(\omega,-\boldsymbol{k}_\parallel,T_1,T_2,T_3)$ if $\tilde{F}^z_{1\to2}(\omega,\boldsymbol{k}_\parallel)\neq\tilde{F}^z_{1\to2}(\omega,-\boldsymbol{k}_\parallel)$ or $\tilde{F}^z_{2\to1}(\omega,\boldsymbol{k}_\parallel)\neq\tilde{F}^z_{2\to1}(\omega,-\boldsymbol{k}_\parallel)$. Below, in a numerical example, we will show that $\tilde{F}^z_{1\to2}(\omega,\boldsymbol{k}_\parallel)\neq\tilde{F}^z_{1\to2}(\omega,-\boldsymbol{k}_\parallel)$ and $\tilde{F}^z_{2\to1}(\omega,\boldsymbol{k}_\parallel)\neq\tilde{F}^z_{2\to1}(\omega,-\boldsymbol{k}_\parallel)$ can occur for both reciprocal and nonreciprocal systems. Therefore, in the nonequilibrium case with $T_1\neq T_2$, $F^z_{1,2}(\omega,\boldsymbol{k}_\parallel,T_1,T_2,T_3)\neq F^z_{1,2}(\omega,-\boldsymbol{k}_\parallel,T_1,T_2,T_3)$ can occur for both reciprocal and nonreciprocal systems.

C. Newton's third law for the Casimir pressure

In our system, both the exterior sides of body 1 and body 2 are covered by perfect electric conductors and hence the system is closed, we have $F^z_{\mathrm{ext},2}=-F^z_{\mathrm{ext},1}$, as shown in Eq. (19). Therefore, from Eqs. (17) and (18), Newton's third law holds for both equilibrium and nonequilibrium pressures at every frequency and in-plane wave vector, i.e.,

$$F^z_1(\omega,\boldsymbol{k}_\parallel,T_1,T_2,T_3)=-F^z_2(\omega,\boldsymbol{k}_\parallel,T_1,T_2,T_3). \tag{31}$$

We emphasize that Newton's third law is in fact distinct from the reciprocity constraints while it has a form that is somewhat similar to some of the constraints associated with reciprocity. It has been reported in Ref. [53] that Newton's third law holds for equilibrium Casimir forces including nonreciprocal materials. Our results here agree with Ref. [53] when specialized to the equilibrium case where $T_1=T_2=T_3$, but generalize the discussion on Newton's third law for nonequilibrium Casimir forces.

D. Numerical verification

In Fig. 2 we provide a detailed numerical verification of the theoretical results as discussed above. For this purpose, we consider three cases.

1. Case 1: Reciprocal case in equilibrium

We first provide a direct check of Eq. (22), which shows the Casimir pressure spectrum is symmetric in $\boldsymbol{k}_\parallel$ space for reciprocal systems. For this purpose, we use the model system as described in Sec. II, with body 2 consisting of the reciprocal anisotropic material as described in Eq. (2).

Figure 2(a) shows exchange function $\tilde{F}^z_{1\to2}(\omega,\boldsymbol{k}_\parallel)$ as a function of ω and $\boldsymbol{k}_\parallel$, for in-plane wave vector $\boldsymbol{k}_\parallel$ that is at an angle of $\varphi=\frac{\pi}{4}$ from the x axis. The choice of the direction of $\boldsymbol{k}_\parallel$ and the reciprocal anisotropic material is such that this system does not have either inversion or mirror symmetry that relates this $\boldsymbol{k}_\parallel$ and $-\boldsymbol{k}_\parallel$. The exchange function, which is proportional to the force component, in general peaks at the dispersion relation of the system, as determined using Eq. (3) with $w=1$. It is attractive (red color) for the frequency range below $0.72\omega_p$, and repulsive (blue color) above the frequency for both $\boldsymbol{k}_\parallel$ and $-\boldsymbol{k}_\parallel$. We emphasize that $\tilde{F}^z_{1\to2}(\omega,\boldsymbol{k}_\parallel)$ is not symmetric, despite the fact that $\tilde{F}^z_{1\to2}(\omega,\boldsymbol{k}_\parallel)$ peaks at the dispersion relation of the surface modes, and the dispersion relation is symmetric for

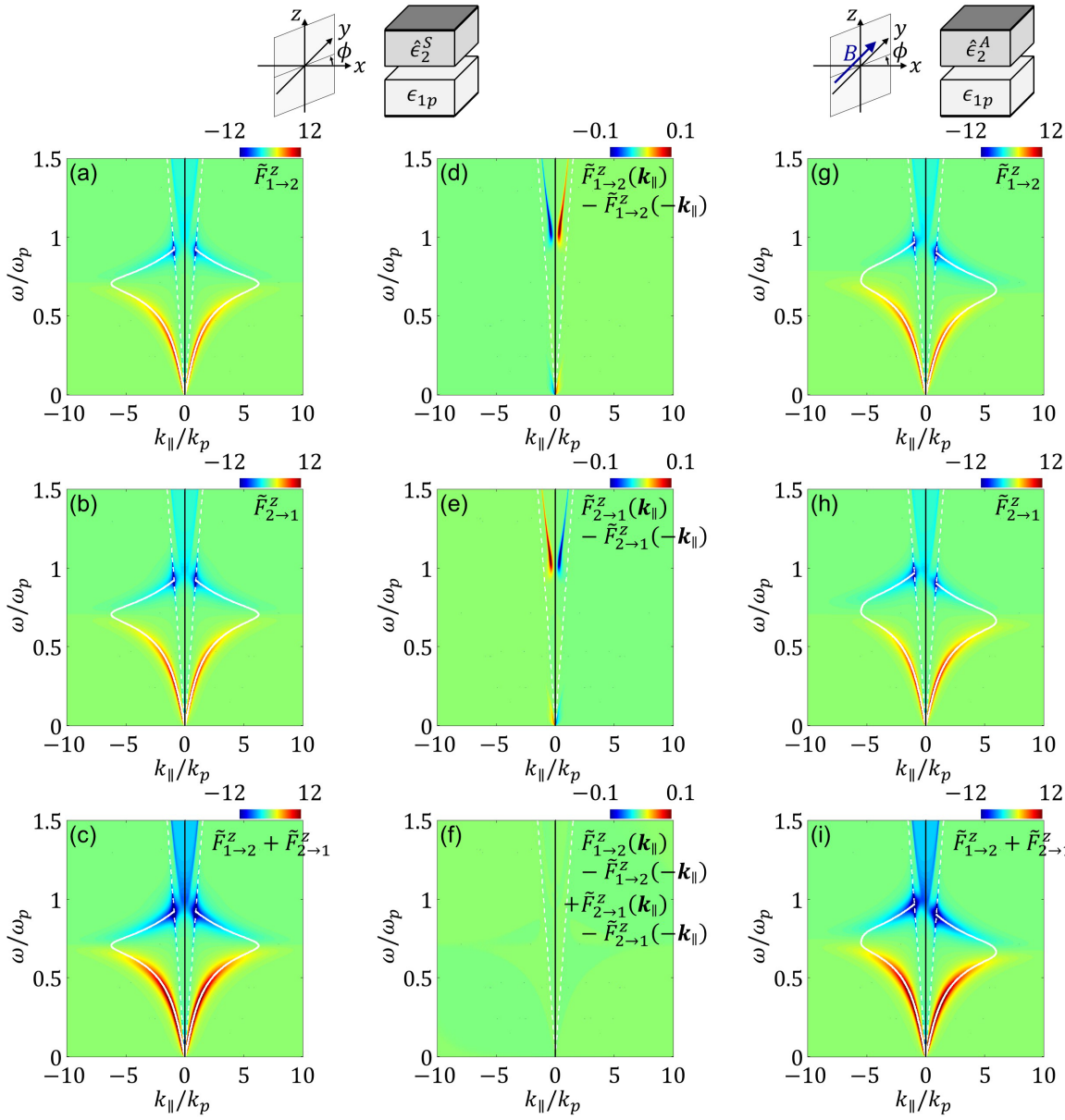

FIG. 2. Spectra of exchange functions for Casimir pressure. (a) $\tilde{F}^z_{1\to2}(\omega,\boldsymbol{k}_\parallel)$, (b) $\tilde{F}^z_{2\to1}(\omega,\boldsymbol{k}_\parallel)$, and (c) summation $\tilde{F}^z_{1\to2}(\omega,\boldsymbol{k}_\parallel)+\tilde{F}^z_{2\to1}(\omega,\boldsymbol{k}_\parallel)$ for reciprocal system with permittivity of body 2 given by $\hat{\epsilon}_2^S$ [Eq. (2)]. Angle of $\varphi=\pi/4$ is selected. (d)–(f) show subtraction $\tilde{F}^z_{l\to m}(\omega,\boldsymbol{k}_\parallel)-\tilde{F}^z_{l\to m}(\omega,-\boldsymbol{k}_\parallel)$ corresponding to (a)–(c), respectively. (g) $\tilde{F}^z_{1\to2}(\omega,\boldsymbol{k}_\parallel)$, (h) $\tilde{F}^z_{2\to1}(\omega,\boldsymbol{k}_\parallel)$, and (i) summation $\tilde{F}^z_{1\to2}(\omega,\boldsymbol{k}_\parallel)+\tilde{F}^z_{2\to1}(\omega,\boldsymbol{k}_\parallel)$ for nonreciprocal system with permittivity of body 2 given by $\hat{\epsilon}_2^A$ [Eq. (1)]. White solid lines represent dispersion curves obtained from Eq. (3) with $w=1$ in (a)–(c) and $w=2$ in (g)–(i), respectively. White dashed lines in each panel represent lightlines.

reciprocal systems [54]. To clearly demonstrate the asymmetric aspect of $\tilde{F}^z_{1\to2}(\omega,\boldsymbol{k}_\parallel)$, we plot $\tilde{F}^z_{1\to2}(\boldsymbol{k}_\parallel)-\tilde{F}^z_{1\to2}(-\boldsymbol{k}_\parallel)$ in Fig. 2(d) for both evanescent and propagation waves, and notice that the plotted values are nonzero. The asymmetric property $\tilde{F}^z_{1\to2}(\boldsymbol{k}_\parallel)\neq\tilde{F}^z_{1\to2}(-\boldsymbol{k}_\parallel)$ comes from $\hat{R}_l(\boldsymbol{k}_\parallel)\neq\hat{R}_l(-\boldsymbol{k}_\parallel)$, which is seen from the comparison of Eqs. (15) and (25). Similar behaviors are observed for $\tilde{F}^z_{2\to1}(\omega,\boldsymbol{k}_\parallel)$, as shown in Figs. 2(b) and 2(e), respectively. On the other hand, the summation $\tilde{F}^z_{1\to2}(\omega,\boldsymbol{k}_\parallel)+\tilde{F}^z_{2\to1}(\omega,\boldsymbol{k}_\parallel)$ [Fig. 2(c)], which relates to forces $F^z_{1,2}(\omega,\boldsymbol{k}_\parallel,T_1,T_2,T_3)$ with $T_1=T_2$, is symmetric, as can be seen by Fig. 2(f), where we plot $\tilde{F}^z_{1\to2}(\boldsymbol{k}_\parallel)-\tilde{F}^z_{1\to2}(-\boldsymbol{k}_\parallel)+\tilde{F}^z_{2\to1}(\boldsymbol{k}_\parallel)-\tilde{F}^z_{2\to1}(-\boldsymbol{k}_\parallel)$, and notice that the plotted values are zero for all ω and $\boldsymbol{k}_\parallel$. The numerical results provide a direct check of Eq. (28), which leads to Eq. (22).

2. *Case 2: Nonreciprocal case in equilibrium*

We next show that Eq. (22) can be violated for nonreciprocal systems at equilibrium. For this purpose, we use the model system as described in Sec. II, with body 2 consisting of the nonreciprocal material as described in Eq. (1). Here, we use the same $\boldsymbol{k}_\parallel$ as in case 1. We numerically investigate the spectra of $\tilde{F}^z_{1\to2}(\omega,\boldsymbol{k}_\parallel)$ and $\tilde{F}^z_{2\to1}(\omega,\boldsymbol{k}_\parallel)$ as shown in Figs. 2(g) and 2(h), respectively, and the summation

$\tilde{F}^z_{1\to2}(\omega,\boldsymbol{k}_\parallel)+\tilde{F}^z_{2\to1}(\omega,\boldsymbol{k}_\parallel)$ in Fig. 2(i). The exchange functions and their summation in general peak at the dispersion relation of the system, as determined using Eq. (3) with $w=2$. Since the dispersion relation for this nonreciprocal system is asymmetric, we see that the spectra in the three panels are asymmetric. And, hence the pressure spectra are asymmetric as well.

3. Case 3: Nonequilibrium cases

We now consider the nonequilibrium cases. Our numerical results in Fig. 2 show that for both reciprocal and nonreciprocal cases, we can have $\tilde{F}^z_{1\to2}(\omega,\boldsymbol{k}_\parallel)\neq\tilde{F}^z_{1\to2}(\omega,-\boldsymbol{k}_\parallel)$. When $T_1\neq T_2$, from the discussion of Eqs. (29) and (30), these numerical results directly indicate that $F^z_{1,2}(\omega,\boldsymbol{k}_\parallel,T_1,T_2,T_3)\neq F^z_{1,2}(\omega,-\boldsymbol{k}_\parallel,T_1,T_2,T_3)$ can hold for both reciprocal and nonreciprocal cases. On the other hand, in the case of $T_1=T_2\neq T_3$ with the behavior given by $\tilde{F}^z_{1\to2}(\omega,\boldsymbol{k}_\parallel)+\tilde{F}^z_{2\to1}(\omega,\boldsymbol{k}_\parallel)$, for the two structures as considered above, we have $F^z_{1,2}(\omega,\boldsymbol{k}_\parallel,T_1,T_2,T_3)=F^z_{1,2}(\omega,-\boldsymbol{k}_\parallel,T_1,T_2,T_3)$ for the reciprocal structure [Figs. 2(c) and 2(f)] and $F^z_{1,2}(\omega,\boldsymbol{k}_\parallel,T_1,T_2,T_3)\neq F^z_{1,2}(\omega,-\boldsymbol{k}_\parallel,T_1,T_2,T_3)$ for the nonreciprocal structure [Fig. 2(i)], as can also be inferred from Eqs. (29) and (30).

IV. LATERAL CASIMIR FORCE

Following the Casimir pressure in the previous section, here we investigate the lateral Casimir force. We present the derivation of the formalism in Sec. IV A, the symmetry properties in Sec. IV B, Newton's third law in Sec. IV C, and numerical verification in Sec. IV D. It is known that independent of whether the bodies are reciprocal or not, the lateral force is always zero in equilibrium [42]. Therefore, in this section we focus only on the nonequilibrium case.

A. Formalism of the lateral Casimir force

We consider the lateral Casimir force $\boldsymbol{F}^\parallel_{1\to2}(\boldsymbol{r}_\parallel,z,t,T_1)$. The lateral force is computed from the electric field $\boldsymbol{E}(\boldsymbol{r}_\parallel,z,t,T_1)$ and the magnetic field $\boldsymbol{H}(\boldsymbol{r}_\parallel,z,t,T_1)$ in the vacuum gap, and has the form

$$\boldsymbol{F}^\parallel_{1\to2}(\boldsymbol{r}_\parallel,z,t,T_1)=\langle\epsilon_0\boldsymbol{E}_\parallel E_z+\mu_0\boldsymbol{H}_\parallel H_z\rangle. \tag{32}$$

From Eqs. (5)–(7) and (32), we have

$$\boldsymbol{F}^\parallel_{1\to2}=\int_0^\infty d\omega\int_{-\infty}^\infty\frac{d\boldsymbol{k}_\parallel}{(2\pi)^4}\boldsymbol{T}^\parallel_{1\to2}(\omega,\boldsymbol{k}_\parallel,T_1), \tag{33}$$

where

$$\boldsymbol{T}^\parallel_{1\to2}(\omega,\boldsymbol{k}_\parallel,T_1)=\tfrac{1}{2}\mathrm{Re}\langle\epsilon_0\boldsymbol{E}_\parallel E_z^*+\mu_0\boldsymbol{H}_\parallel H_z^*\rangle. \tag{34}$$

Substituting the electric field of Eq. (7) and the corresponding magnetic field into Eq. (34), we have the forms of the stress tensor for propagation and evanescent waves, respectively, as

$$\boldsymbol{T}^\parallel_{1\to2}(\omega,\boldsymbol{k}_\parallel,T_1)=\begin{cases}\boldsymbol{k}_\parallel\mathrm{Tr}\big[-\frac{1}{2Z\omega}(\hat{I}-\hat{R}_2^\dagger\hat{R}_2)\hat{D}_{12}\langle\boldsymbol{E}_1\boldsymbol{E}_1^\dagger\rangle\hat{D}_{12}^\dagger\big], & (k_\parallel<k_0)\\ \boldsymbol{k}_\parallel\mathrm{Tr}\big[-\frac{1}{2Z\omega}(\hat{R}_2^\dagger-\hat{R}_2)\hat{D}_{12}\langle\boldsymbol{E}_1\boldsymbol{E}_1^\dagger\rangle\hat{D}_{12}^\dagger e^{-2\kappa_{z0}d}\big]. & (k_\parallel>k_0)\end{cases} \tag{35}$$

From Eqs. (13), (33), and (35), we have the lateral force from body 1 to body 2:

$$\boldsymbol{F}^\parallel_{1\to2}(\omega,\boldsymbol{k}_\parallel,T_1)=\left[n(\omega,T_1)+\frac{1}{2}\right]\frac{\hbar\boldsymbol{k}_\parallel}{8\pi^3}\tilde{F}^\parallel_{1\to2}(\omega,\boldsymbol{k}_\parallel), \tag{36}$$

where

$$\tilde{F}^\parallel_{l\to m}(\omega,\boldsymbol{k}_\parallel)=\begin{cases}\mathrm{Tr}[(-1)^l(\hat{I}-\hat{R}_m^\dagger\hat{R}_m)\hat{D}_{lm}(\hat{I}-\hat{R}_l\hat{R}_l^\dagger)\hat{D}_{lm}^\dagger], & (k_\parallel<k_0)\\ \mathrm{Tr}[(-1)^l(\hat{R}_m^\dagger-\hat{R}_m)\hat{D}_{lm}(\hat{R}_l-\hat{R}_l^\dagger)\hat{D}_{lm}^\dagger e^{-2\kappa_{z0}d}], & (k_\parallel>k_0)\end{cases} \tag{37}$$

again $(l,m)=(1,2),(2,1)$. The factor of $(-1)^l$ arises from the definition of the reflection matrices. We note that the exchange function $\tilde{F}^\parallel_{1\to2}(\omega,\boldsymbol{k}_\parallel)$ for the lateral force [Eq. (37)] is the same as that for the heat transfer derived in Refs. [50,55], as was noted in Ref. [42]. The exchange function $\tilde{F}^\parallel_{1\to2}(\omega,\boldsymbol{k}_\parallel)$ for the lateral force also has a similar form as the exchange function $\tilde{F}^z_{1\to2}(\omega,\boldsymbol{k}_\parallel)$ for the pressure [Eq. (15)], except for the sign flip of the term relating reflection matrix $\hat{R}_2$ for body 2, i.e., $\hat{I}+\hat{R}_2^\dagger\hat{R}_2$ for propagation waves and $\hat{R}_2^\dagger+\hat{R}_2$ for evanescent waves in Eq. (15). The total lateral forces acting on bodies 1 and 2 are given by

$$\boldsymbol{F}^\parallel_{1,2}(T_1,T_2)=\int_0^\infty d\omega\int_{-\infty}^\infty d\boldsymbol{k}_\parallel\boldsymbol{F}^\parallel_{1,2}(\omega,\boldsymbol{k}_\parallel,T_1,T_2), \tag{38}$$

where

$$\boldsymbol{F}^\parallel_1(\omega,\boldsymbol{k}_\parallel,T_1,T_2)=\boldsymbol{F}^\parallel_{1\to2}(\omega,\boldsymbol{k}_\parallel,T_1)+\boldsymbol{F}^\parallel_{2\to1}(\omega,\boldsymbol{k}_\parallel,T_2), \tag{39}$$

$$\boldsymbol{F}^\parallel_2(\omega,\boldsymbol{k}_\parallel,T_1,T_2)=-\boldsymbol{F}^\parallel_{1\to2}(\omega,\boldsymbol{k}_\parallel,T_1)-\boldsymbol{F}^\parallel_{2\to1}(\omega,\boldsymbol{k}_\parallel,T_2). \tag{40}$$

We note that there is no component of the lateral force at exterior boundaries A and C due to the plates of perfect electric conductor. In deriving Eqs. (39) and (40), similarly, we have used the relation

$$\boldsymbol{F}^\parallel_{1\to1}(\omega,\boldsymbol{k}_\parallel,T_1)=-\boldsymbol{F}^\parallel_{1\to2}(\omega,\boldsymbol{k}_\parallel,T_1), \tag{41}$$

$$\boldsymbol{F}^\parallel_{2\to2}(\omega,\boldsymbol{k}_\parallel,T_2)=-\boldsymbol{F}^\parallel_{2\to1}(\omega,\boldsymbol{k}_\parallel,T_2). \tag{42}$$

B. Symmetry properties for the lateral Casimir force

Following the formalism in the previous section, we discuss symmetry properties of the lateral Casimir force in the $\boldsymbol{k}_\parallel$ space. Similar to Sec. III B, here we focus on the relation between the lateral force at $\boldsymbol{k}_\parallel$ and at $-\boldsymbol{k}_\parallel$. We show that a similar reciprocity constraint is present for the lateral Casimir force as well.

As the second main result of the paper, we show for the reciprocal system the spectra of the lateral force acting on each of bodies 1 and 2 are symmetric with respect to $\boldsymbol{k}_\parallel$:

$$\boldsymbol{F}^\parallel_{1,2}(\omega,\boldsymbol{k}_\parallel,T_1,T_2)=-\boldsymbol{F}^\parallel_{1,2}(\omega,-\boldsymbol{k}_\parallel,T_1,T_2). \tag{43}$$

We prove Eq. (43) from Eqs. (39) and (40) via the examination of the exchange functions. From the relation of the reflection matrix for the reciprocal system [Eq. (23)] and the

exchange function [Eq. (37)], we have

$$\tilde{F}^{\parallel}_{1\to 2}(\omega, -\boldsymbol{k}_{\parallel}) = -\tilde{F}^{\parallel}_{2\to 1}(\omega, \boldsymbol{k}_{\parallel}). \tag{44}$$

The detailed deviation is found in Appendix B. In addition, regardless of whether the system is nonreciprocal or reciprocal, the exchange function for the lateral forces is symmetric with respect to an exchange of bodies 1 and 2, i.e.,

$$\tilde{F}^{\parallel}_{1\to 2}(\omega, \boldsymbol{k}_{\parallel}) = -\tilde{F}^{\parallel}_{2\to 1}(\omega, \boldsymbol{k}_{\parallel}). \tag{45}$$

The detailed derivation is found in Appendix C. Both of these derivations parallel those of the related results for heat transfer in Ref. [50]. From Eqs. (44) and (45), we have the relation of symmetry in the spectrum

$$\tilde{F}^{\parallel}_{1\to 2}(\omega, \boldsymbol{k}_{\parallel}) = \tilde{F}^{\parallel}_{1\to 2}(\omega, -\boldsymbol{k}_{\parallel}). \tag{46}$$

Equations (44) to (46) are true by exchanging the subscripts 1 and 2. From Eqs. (36), (39), and (40), we have

$$\boldsymbol{F}^{\parallel}_{1}(\omega, \boldsymbol{k}_{\parallel}, T_1, T_2) = \left[n(\omega, T_1) + \frac{1}{2}\right]\frac{\hbar \boldsymbol{k}_{\parallel}}{8\pi^3}\tilde{F}^{\parallel}_{1\to 2}(\omega, \boldsymbol{k}_{\parallel}) + \left[n(\omega, T_2) + \frac{1}{2}\right]\frac{\hbar \boldsymbol{k}_{\parallel}}{8\pi^3}\tilde{F}^{\parallel}_{2\to 1}(\omega, \boldsymbol{k}_{\parallel}), \tag{47}$$

and

$$\boldsymbol{F}^{\parallel}_{2}(\omega, \boldsymbol{k}_{\parallel}, T_1, T_2) = -\left[n(\omega, T_1) + \frac{1}{2}\right]\frac{\hbar \boldsymbol{k}_{\parallel}}{8\pi^3}\tilde{F}^{\parallel}_{1\to 2}(\omega, \boldsymbol{k}_{\parallel}) - \left[n(\omega, T_2) + \frac{1}{2}\right]\frac{\hbar \boldsymbol{k}_{\parallel}}{8\pi^3}\tilde{F}^{\parallel}_{2\to 1}(\omega, \boldsymbol{k}_{\parallel}). \tag{48}$$

From Eqs. (47) and (48), one can clearly check that the lateral forces $\boldsymbol{F}^{\parallel}_{1,2}(\omega, \boldsymbol{k}_{\parallel}, T_1, T_2)$ are symmetric if and only if exchange functions $\tilde{F}^{\parallel}_{1\to 2}(\boldsymbol{k}_{\parallel}, \omega)$ and $\tilde{F}^{\parallel}_{2\to 1}(\boldsymbol{k}_{\parallel}, \omega)$ are symmetric. Hence, from Eq. (46), Eq. (43) has been proved. We also observe from Eqs. (45), (47), and (48) that the lateral force becomes zero in equilibrium. Our observation agrees with Refs. [42,45], but contradicts the results in Ref. [56], where nonzero lateral force in equilibrium was claimed. References [42,45] have argued that the lateral force in equilibrium should be zero, as expected from a general thermodynamics consideration.

C. Newton's third law for the lateral Casimir force

Similar to the pressure, from Eqs. (39) and (40), Newton's third law holds for the lateral forces at every frequency and in-plane wave vector, as long as no exchange of photons occurs between the two-body system and the environment.

$$\boldsymbol{F}^{\parallel}_{1}(\omega, \boldsymbol{k}_{\parallel}, T_1, T_2) = -\boldsymbol{F}^{\parallel}_{2}(\omega, \boldsymbol{k}_{\parallel}, T_1, T_2). \tag{49}$$

D. Numerical verification

In Fig. 3 we provide a detailed numerical verification of Eq. (43) by considering two cases in nonequilibrium. In these examples, the lateral force is along the x direction and we plot the dependency of exchange functions, which control the behavior of $\boldsymbol{F}^{\parallel}_{1,2}$ on the parallel wave vector along the direction, $\varphi = \frac{\pi}{4}$.

1. Case 1: Reciprocal case

We provide a direct check of Eq. (43), which shows the lateral force spectrum is symmetric in $\boldsymbol{k}_{\parallel}$ space for reciprocal systems. For this purpose, we use the model system as described in Sec. II, with body 2 consisting of the reciprocal anisotropic material as described in Eq. (2).

Figure 3(a) shows the spectrum of exchange function $\tilde{F}^{\parallel}_{1\to 2}(\omega, \boldsymbol{k}_{\parallel})$ for this reciprocal case. $\tilde{F}^{\parallel}_{1\to 2}(\omega, \boldsymbol{k}_{\parallel})$ peaks at the dispersion curves (white solid lines) obtained from Eq. (3) with $w = 1$ as overlaid in Fig. 3(a). $\tilde{F}^{\parallel}_{1\to 2}(\omega, \boldsymbol{k}_{\parallel})$ is negative (blue color) for the entire area of $(\omega, \boldsymbol{k}_{\parallel})$ we consider here. The spectrum of $\tilde{F}^{\parallel}_{1\to 2}(\omega, \boldsymbol{k}_{\parallel})$ is symmetric, as can be clearly seen in Fig. 3(c), where we plot $\tilde{F}^{\parallel}_{1\to 2}(\boldsymbol{k}_{\parallel}) - \tilde{F}^{\parallel}_{1\to 2}(-\boldsymbol{k}_{\parallel})$ and show that plotted values are zero for all ω and $\boldsymbol{k}_{\parallel}$. This result here contrasts with exchange function $\tilde{F}^{z}_{1\to 2}(\omega, \boldsymbol{k}_{\parallel})$ for the pressure, which is asymmetric as plotted in Figs. 2(a) and 2(d). Figures 3(b) and 3(d) show $\tilde{F}^{\parallel}_{2\to 1}(\omega, \boldsymbol{k}_{\parallel})$, where it has a positive value and the same symmetric properties as $\tilde{F}^{\parallel}_{1\to 2}(\omega, \boldsymbol{k}_{\parallel})$. Therefore, the symmetry property of the lateral force spectrum in the reciprocal system [Eq. (43)] is verified.

2. Case 2: Nonreciprocal case

We next show that Eq. (43) can be violated for nonreciprocal systems. For this purpose, we use the model system as described in Sec. II, with body 2 consisting of the nonreciprocal material as described in Eq. (1). We plot the spectra of exchange functions $\tilde{F}^{\parallel}_{1\to 2}(\omega, \boldsymbol{k}_{\parallel})$ and $\tilde{F}^{\parallel}_{2\to 1}(\omega, \boldsymbol{k}_{\parallel})$ in Figs. 3(e) and 3(f), respectively. Both $\tilde{F}^{\parallel}_{1\to 2}(\omega, \boldsymbol{k}_{\parallel})$ and $\tilde{F}^{\parallel}_{2\to 1}(\omega, \boldsymbol{k}_{\parallel})$ peak at the dispersion relation of the surface modes, as calculated using Eq. (3) with $w = 2$, and overlaid in the figures. Since the dispersion relation for such nonreciprocal system is asymmetric, the exchange functions are asymmetric with respect to $\boldsymbol{k}_{\parallel}$ as well.

It is noted that the main results of Eqs. (22) and (43) for the pressure and lateral force hold for any reciprocal material satisfying Eq. (23), including uniaxial materials with arbitral direction of the optical axis, although the permittivity of Eq. (2) has been used as an illustration.

V. CONCLUSIONS

We have investigated the Casimir pressure and lateral force in the two-plate system, where one of the plates consists of a reciprocal anisotropic or nonreciprocal material. Our analytical and numerical results have revealed a distinct signature of reciprocity in the equilibrium pressure and the nonequilibrium lateral force, where the spectra are symmetric with respect to $\boldsymbol{k}_{\parallel}$. On the other hand, for the nonequilibrium pressure, the spectra may be asymmetric for both reciprocal and nonreciprocal cases. In addition, we have shown that Newton's third law holds for every frequency and wave vector, as long as no exchange of photons occurs between the two-body system and the environment. Our results provide understandings of some of the symmetry properties of Casimir pressures and lateral forces in equilibrium or nonequilibrium for reciprocal or nonreciprocal systems.

In our study, here we assume that the two bodies are stationery with respect one another. It should be of interest to

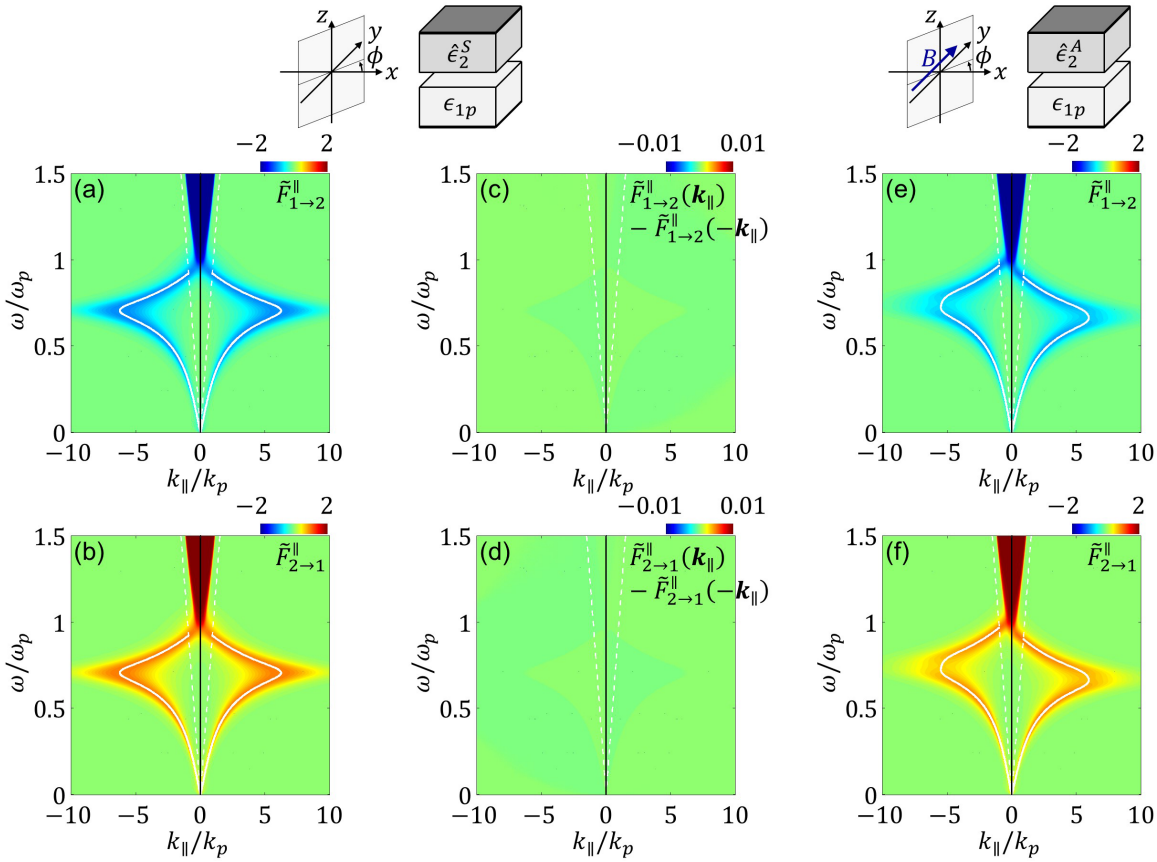

FIG. 3. Spectra of exchange functions for lateral Casimir force. (a) $\tilde{F}^{\parallel}_{1\to2}(\omega, \boldsymbol{k}_\parallel)$ and (b) $\tilde{F}^{\parallel}_{2\to1}(\omega, \boldsymbol{k}_\parallel)$ for reciprocal system with permittivity of body 2 given by $\hat{\epsilon}_2^S$ [Eq. (2)]. Angle of $\varphi = \pi/4$ is selected. (c) and (d) show the subtraction $\tilde{F}^{\parallel}_{l\to m}(\omega, \boldsymbol{k}_\parallel) - \tilde{F}^{\parallel}_{l\to m}(\omega, -\boldsymbol{k}_\parallel)$ corresponding to (a) and (b), respectively. (e) $\tilde{F}^{\parallel}_{1\to2}(\omega, \boldsymbol{k}_\parallel)$ and (f) $\tilde{F}^{\parallel}_{2\to1}(\omega, \boldsymbol{k}_\parallel)$ for the nonreciprocal system with the permittivity of body 2 given by $\hat{\epsilon}_2^A$ [Eq. (1)]. White solid lines represent dispersion curves obtained from Eq. (3) with $w = 1$ in (a) and (b) and $w = 2$ in (e) and (f), respectively. White dashed lines in each panel represent lightlines.

generalize our results to the case where the two bodies are in relative motion [46].

ACKNOWLEDGMENT

S.F.'s contribution to this publication was as a consultant, and was not part of his Stanford duties or responsibilities as a professor.

APPENDIX A: DERIVATION OF DISPERSION EQUATION OF EQ. (3)

Dispersion relations of the surface modes in a three-layer structure including an anisotropic planar body are presented in Ref. [57]. Here, we include the effect of twist of the anisotropic planar body in the dispersion relations. We consider p-polarized evanescent waves in the system of Fig. 1(a). The permittivities $\hat{\epsilon}_2^A$ in Eq. (1) and $\hat{\epsilon}_2^S$ in Eq. (2) have the form

$$\hat{\epsilon}_2 = \begin{pmatrix} \epsilon_d & 0 & \epsilon_{xz} \\ 0 & \epsilon_p & 0 \\ \epsilon_{zx} & 0 & \epsilon_d \end{pmatrix}. \tag{A1}$$

The dispersion relation of the surface modes for in-plane wave vector $\boldsymbol{k}_\parallel$ that is at angle φ from the x axis is equivalent to that for wave vector $\boldsymbol{k_x}$ with the twist of the anisotropic planar body by angle $-\varphi$. Thus, the permittivity of the twisted anisotropic planar body is given by

$$\hat{\epsilon}_2^{'} = \hat{R}_z \hat{\epsilon}_2 \hat{R}_z^{\dagger} = \begin{pmatrix} \epsilon_d \cos^2(\varphi) + \epsilon_p \sin^2(\varphi) & -(\epsilon_d - \epsilon_p)\sin(\varphi)\cos(\varphi) & \epsilon_{xz}\cos(\varphi) \\ -(\epsilon_d - \epsilon_p)\sin(\varphi)\cos(\varphi) & \epsilon_d \sin^2(\varphi) + \epsilon_p \cos^2(\varphi) & -\epsilon_{xz}\sin(\varphi) \\ \epsilon_{zx}\cos(\varphi) & -\epsilon_{zx}\sin(\varphi) & \epsilon_d \end{pmatrix}, \tag{A2}$$

where

$$\hat{R}_z = \begin{pmatrix} \cos(-\varphi) & -\sin(-\varphi) & 0 \\ \sin(-\varphi) & \cos(-\varphi) & 0 \\ 0 & 0 & 1 \end{pmatrix}. \tag{A3}$$

The regions of the vacuum gap, body 1, and body 2 are labeled by 0, 1, and 2, respectively. The magnetic fields for the three regions are given by

$$H_{0,y} = H_{0,y}^{+} e^{ik_x x - \kappa_{z0} z} + H_{0,y}^{-} e^{ik_x x + \kappa_{z0}(z-d)}, \tag{A4}$$

$$H_{1,y} = H_{1,y}^{-} e^{ik_x x + \kappa_{z1} z}, \tag{A5}$$

$$H_{2,y} = H_{2,y}^{+} e^{ik_x x - \kappa_{z2}(z-d)}, \tag{A6}$$

where the superscripts + and − of the y component of the magnetic field represent the upward and downward waves along the z axis. The electric fields are, correspondingly, given by

$$E_{0,x} = \frac{\kappa_{z0}}{i\omega\epsilon_0}(-H_{0,y}^{+} e^{ik_x x - \kappa_{z0} z} + H_{0,y}^{-} e^{ik_x x + \kappa_{z0}(z-d)}), \tag{A7}$$

$$\epsilon_p E_{1,x} = \frac{\kappa_{z1}}{i\omega\epsilon_0} H_{1,y}^{-} e^{ik_x x + \kappa_{z1} z}, \tag{A8}$$

$$(\epsilon_d \cos^2(\varphi) + \epsilon_p \sin^2(\varphi)) E_{2,x} + \epsilon_{xz} \cos(\varphi) E_{2,z} = -\frac{\kappa_{z2}}{i\omega\epsilon_0} H_{2,y}^{+} e^{ik_x x - \kappa_{z2}(z-d)}, \tag{A9}$$

$$\epsilon_{zx} \cos(\varphi) E_{2,x} + \epsilon_d E_{2,z} = -\frac{k_x}{\omega\epsilon_0} H_{2,y}^{+} e^{ik_x x - \kappa_{z2}(z-d)}. \tag{A10}$$

The boundary conditions are

$$H_{0,y}|_{z=0} = H_{1,y}|_{z=0}, \tag{A11}$$

$$E_{0,x}|_{z=0} = E_{1,x}|_{z=0}, \tag{A12}$$

$$H_{0,y}|_{z=d} = H_{2,y}|_{z=d}, \tag{A13}$$

$$E_{0,x}|_{z=d} = E_{2,x}|_{z=d}. \tag{A14}$$

From Eqs. (A4)–(A14), the dispersion equation is derived:

$$\left(\frac{\frac{\epsilon_d^2 - \epsilon_{xz}\epsilon_{zx}}{\epsilon_d}\cos^2(\varphi) + \epsilon_p \sin^2(\varphi)}{\kappa_{z2}} + \frac{1}{\kappa_{z0}} - i\frac{\frac{\epsilon_{xz}}{\epsilon_d}k_x \cos(\varphi)}{\kappa_{z0}\kappa_{z2}}\right)\left(\frac{\epsilon_p}{\kappa_{z1}} + \frac{1}{\kappa_{z0}}\right)e^{\kappa_{z0} d}$$
$$- \left(\frac{\frac{\epsilon_d^2 - \epsilon_{xz}\epsilon_{zx}}{\epsilon_d}\cos^2(\varphi) + \epsilon_p \sin^2(\varphi)}{\kappa_{z2}} - \frac{1}{\kappa_{z0}} + i\frac{\frac{\epsilon_{xz}}{\epsilon_d}k_x \cos(\varphi)}{\kappa_{z0}\kappa_{z2}}\right)\left(\frac{\epsilon_p}{\kappa_{z1}} - \frac{1}{\kappa_{z0}}\right)e^{-\kappa_{z0} d} = 0, \tag{A15}$$

where $\epsilon_{xz} = \epsilon_{zx} = \epsilon_f$ for the reciprocal system, and $\epsilon_{xz} = -\epsilon_{zx} = i\epsilon_f$ for the nonreciprocal system. Equation (A15) is recovered to Eq. (6B) in Ref. [57] with $\varphi = 0$ (Voigt configuration) for a nonreciprocal system. κ_{z2} is obtained from solving for $\nabla \times \nabla \times \boldsymbol{E} - \omega^2 \mu_0 \epsilon_0 \hat{\epsilon}_2' \boldsymbol{E} = 0$, which is given by

$$\kappa_{z2}^4 - ik_x \frac{\epsilon_{xz} + \epsilon_{zx}}{\epsilon_d}\cos(\varphi)\kappa_{z2}^3 + \left[-\left(1 + \cos^2(\varphi) + \frac{\epsilon_p}{\epsilon_d}\sin^2(\varphi)\right)k_x^2 + \left(\epsilon_p + \epsilon_d - \frac{\epsilon_{xz}\epsilon_{zx}}{\epsilon_d}\right)k_0^2\right]\kappa_{z2}^2$$
$$+ i\left(k_x^2 - \epsilon_p k_0^2\right)k_x \frac{\epsilon_{xz} + \epsilon_{zx}}{\epsilon_d}\cos(\varphi)\kappa_{z2} + \left(\cos^2(\varphi) + \frac{\epsilon_p}{\epsilon_d}\sin^2(\varphi)\right)k_x^4 + \left[-\left(\epsilon_d + \epsilon_p - \frac{\epsilon_{xz}\epsilon_{zx}}{\epsilon_d}\right)\cos^2(\varphi) - 2\epsilon_p \sin^2(\varphi)\right]k_x^2 k_0^2$$
$$+ \epsilon_p\left(\epsilon_d - \frac{\epsilon_{xz}\epsilon_{zx}}{\epsilon_d}\right)k_0^4 = 0. \tag{A16}$$

One can check that in the case of $\varphi = 0$ in the nonreciprocal system with $\epsilon_{xz} = -\epsilon_{zx} = i\epsilon_f$, Eq. (A16) gives $\kappa_{z2} = \sqrt{k_x^2 - \frac{\epsilon_d^2 - \epsilon_f^2}{\epsilon_d}k_0^2}$ and $\sqrt{k_x^2 - \epsilon_p k_0^2}$ [57].

APPENDIX B: PROOF OF EQ. (44)

Substituting Eq. (23) into Eq. (37), $\tilde{F}_{1\to2}^{\parallel}(\omega, \boldsymbol{k}_\parallel)$ is given for propagation waves:

$$\begin{aligned}
\tilde{F}_{1\to2}^{\parallel}(-\boldsymbol{k}_\parallel) &= \mathrm{Tr}[-(\hat{I} - \hat{R}_2^{\dagger}(-\boldsymbol{k}_\parallel)\hat{R}_2(-\boldsymbol{k}_\parallel))\hat{D}_{12}(-\boldsymbol{k}_\parallel)(\hat{I} - \hat{R}_1(-\boldsymbol{k}_\parallel)\hat{R}_1^{\dagger}(-\boldsymbol{k}_\parallel))\hat{D}_{12}^{\dagger}(-\boldsymbol{k}_\parallel)] \\
&= \mathrm{Tr}\big[-\hat{\sigma}_z\big(\hat{I} - \hat{R}_2^{*}(\boldsymbol{k}_\parallel)\hat{R}_2^{T}(\boldsymbol{k}_\parallel)\big)\hat{D}_{21}^{T}(\boldsymbol{k}_\parallel)(\hat{I} - \hat{R}_1^{T}(\boldsymbol{k}_\parallel)\hat{R}_1^{*}(\boldsymbol{k}_\parallel))\hat{D}_{21}^{*}(\boldsymbol{k}_\parallel)\hat{\sigma}_z\big] \\
&= \mathrm{Tr}\big[-\hat{D}_{21}^{*}(\boldsymbol{k}_\parallel)\big(\hat{I} - \hat{R}_2^{*}(\boldsymbol{k}_\parallel)\hat{R}_2^{T}(\boldsymbol{k}_\parallel)\big)\hat{D}_{21}^{T}(\boldsymbol{k}_\parallel)(\hat{I} - \hat{R}_1^{T}(\boldsymbol{k}_\parallel)\hat{R}_1^{*}(\boldsymbol{k}_\parallel))\big]^{T} \\
&= \mathrm{Tr}[-(\hat{I} - \hat{R}_1^{\dagger}(\boldsymbol{k}_\parallel)\hat{R}_1(\boldsymbol{k}_\parallel))\hat{D}_{21}(\boldsymbol{k}_\parallel)(\hat{I} - \hat{R}_2(\boldsymbol{k}_\parallel)\hat{R}_2^{\dagger}(\boldsymbol{k}_\parallel))\hat{D}_{21}^{\dagger}(\boldsymbol{k}_\parallel)] \\
&= -\tilde{F}_{2\to1}^{\parallel}(\boldsymbol{k}_\parallel),
\end{aligned} \tag{B1}$$

where we have used $\mathrm{Tr}[\hat{\sigma}_z\hat{\sigma}_z] = \mathrm{Tr}[\hat{I}]$ and $\mathrm{Tr}[\hat{M}^T] = \mathrm{Tr}[\hat{M}]$ for a matrix $\hat{M}$. Likewise, for evanescent waves, $\tilde{F}_{1\to2}^{\parallel}(\omega, \boldsymbol{k}_\parallel)$ is given:

$$\begin{aligned}
\tilde{F}_{1\to2}^{\parallel}(-\boldsymbol{k}_\parallel) &= \mathrm{Tr}[-(\hat{R}_2^{\dagger}(-\boldsymbol{k}_\parallel) - \hat{R}_2(-\boldsymbol{k}_\parallel))\hat{D}_{12}(-\boldsymbol{k}_\parallel)(\hat{R}_1(-\boldsymbol{k}_\parallel) - \hat{R}_1^{\dagger}(-\boldsymbol{k}_\parallel))\hat{D}_{12}^{\dagger}(-\boldsymbol{k}_\parallel)e^{-2\kappa_{z0}d}] \\
&= \mathrm{Tr}\big[-\hat{\sigma}_z\big(\hat{R}_2^{*}(\boldsymbol{k}_\parallel) - \hat{R}_2^{T}(\boldsymbol{k}_\parallel)\big)\hat{D}_{21}^{T}(\boldsymbol{k}_\parallel)\big(\hat{R}_1^{T}(\boldsymbol{k}_\parallel) - \hat{R}_1^{*}(\boldsymbol{k}_\parallel)\big)\hat{D}_{21}^{*}(\boldsymbol{k}_\parallel)e^{-2\kappa_{z0}d}\hat{\sigma}_z\big] \\
&= \mathrm{Tr}\big[-\hat{D}_{21}^{*}(\boldsymbol{k}_\parallel)\big(\hat{R}_2^{*}(\boldsymbol{k}_\parallel) - \hat{R}_2^{T}(\boldsymbol{k}_\parallel)\big)\hat{D}_{21}^{T}(\boldsymbol{k}_\parallel)\big(\hat{R}_1^{T}(\boldsymbol{k}_\parallel) - \hat{R}_1^{*}(\boldsymbol{k}_\parallel)\big)e^{-2\kappa_{z0}d}\big]^{T} \\
&= \mathrm{Tr}[-(\hat{R}_1^{\dagger}(\boldsymbol{k}_\parallel) - \hat{R}_1(\boldsymbol{k}_\parallel))\hat{D}_{21}(\boldsymbol{k}_\parallel)(\hat{R}_2(\boldsymbol{k}_\parallel) - \hat{R}_2^{\dagger}(\boldsymbol{k}_\parallel))\hat{D}_{21}^{\dagger}(\boldsymbol{k}_\parallel)e^{-2\kappa_{z0}d}] \\
&= -\tilde{F}_{2\to1}^{\parallel}(\boldsymbol{k}_\parallel).
\end{aligned} \tag{B2}$$

APPENDIX C: PROOF OF EQ. (45)

From Eq. (37), exchange function $\tilde{F}^{\parallel}_{1\to 2}(\omega, \boldsymbol{k}_{\parallel})$ for the lateral force is rewritten for propagation waves:

$$\begin{aligned}\tilde{F}^{\parallel}_{1\to 2}(\boldsymbol{k}_{\parallel}) &= \mathrm{Tr}[-(\hat{I}-\hat{R}_2^{\dagger}\hat{R}_2)\hat{D}_{12}(\hat{I}-\hat{R}_1\hat{R}_1^{\dagger})\hat{D}_{12}^{\dagger}]\\ &= \mathrm{Tr}[\hat{R}_2^{\dagger}\hat{R}_2\hat{D}_{12}\hat{D}_{12}^{\dagger}+\hat{D}_{12}\hat{R}_1\hat{R}_1^{\dagger}\hat{D}_{12}^{\dagger}-\hat{R}_2^{\dagger}\hat{R}_2\hat{D}_{12}\hat{R}_1\hat{R}_1^{\dagger}\hat{D}_{12}^{\dagger}-\hat{D}_{12}\hat{D}_{12}^{\dagger}]\\ &= \mathrm{Tr}[\hat{R}_2\hat{D}_{12}(\hat{R}_2\hat{D}_{12})^{\dagger}+\hat{R}_1\hat{D}_{21}(\hat{R}_1\hat{D}_{21})^{\dagger}-\hat{R}_2\hat{D}_{12}\hat{R}_1(\hat{R}_2\hat{D}_{12}\hat{R}_1)^{\dagger}-\hat{R}_1\hat{D}_{21}\hat{R}_2(\hat{R}_1\hat{D}_{21}\hat{R}_2)^{\dagger}\\ &\quad -\hat{R}_1\hat{D}_{21}\hat{R}_2e^{i2k_{0z}d}-(\hat{R}_1\hat{D}_{21}\hat{R}_2e^{i2k_{0z}d})^{\dagger}-\hat{I}], \quad (k_{\parallel}<k_0)\end{aligned} \tag{C1}$$

and for evanescent waves:

$$\begin{aligned}\tilde{F}^{\parallel}_{1\to 2}(\boldsymbol{k}_{\parallel}) &= \mathrm{Tr}[-(\hat{R}_2^{\dagger}-\hat{R}_2)\hat{D}_{12}(\hat{R}_1-\hat{R}_1^{\dagger})\hat{D}_{12}^{\dagger}e^{-2\kappa_{z0}d}]\\ &= \mathrm{Tr}[-\hat{R}_2^{\dagger}\hat{D}_{12}\hat{R}_1\hat{D}_{12}^{\dagger}-\hat{R}_2\hat{D}_{12}\hat{R}_1^{\dagger}\hat{D}_{12}^{\dagger}+\hat{R}_2\hat{D}_{12}\hat{R}_1\hat{D}_{12}^{\dagger}+\hat{R}_2^{\dagger}\hat{D}_{12}\hat{R}_1^{\dagger}\hat{D}_{12}^{\dagger}]e^{-2\kappa_{z0}d}\\ &= \mathrm{Tr}[-\hat{D}_{12}\hat{R}_1(\hat{R}_2\hat{D}_{12})^{\dagger}e^{-2\kappa_0 d}-\hat{D}_{21}\hat{R}_2(\hat{R}_1\hat{D}_{21})^{\dagger}e^{-2\kappa_{z0}d}+\hat{D}_{21}\hat{D}_{12}^{\dagger}+\hat{D}_{12}\hat{D}_{21}^{\dagger}-\hat{D}_{12}-\hat{D}_{12}^{\dagger}].(k_{\parallel}>k_0)\end{aligned} \tag{C2}$$

From Eqs. (C1) and (C2) with the relations of $\mathrm{Tr}\lceil\hat{R}_1\hat{D}_{21}\hat{R}_2\rceil = \mathrm{Tr}\lceil\hat{R}_2\hat{D}_{12}\hat{R}_1\rceil$ and $\mathrm{Tr}\lceil\hat{D}_{12}\rceil = \mathrm{Tr}\lceil\hat{D}_{21}\rceil$, we see that $\tilde{F}^{\parallel}_{1\to 2}(\omega, \boldsymbol{k}_{\parallel})$ is symmetric with respect to bodies 1 and 2, where the minus sign is added for the exchange of the labels of bodies, i.e., $-\tilde{F}^{\parallel}_{2\to 1}(\omega, \boldsymbol{k}_{\parallel})$. Therefore, Eq. (45) has been proved.

[1] H. B. G. Casimir, On the attraction between two perfectly conducting plates, Proc. Kon. Ned. Akad. Wet. **51**, 793 (1948).

[2] E. M. Lifshitz, The theory of molecular attractive forces between solids, Sov. Phys. **2**, 73 (1956).

[3] A. W. Rodriguez, F. Capasso, and S. G. Johnson, The Casimir effect in microstructured geometries, Nat. Photonics **5**, 211 (2011).

[4] T. Gong, M. R. Corrado, A. R. Mahbub, C. Shelden, and J. N. Munday, Recent progress in engineering the Casimir effect - applications to nanophotonics, nanomechanics, and chemistry, Nanophotonics **10**, 523 (2021).

[5] S. K. Lamoreaux, Demonstration of the Casimir Force in the 0.6 to 6 μm Range, Phys. Rev. Lett. **78**, 5 (1997).

[6] G. Bressi, G. Carugno, R. Onofrio, and G. Ruoso, Measurement of the Casimir Force between Parallel Metallic Surfaces, Phys. Rev. Lett. **88**, 041804 (2002).

[7] J. N. Munday, F. Capasso, and A. Parsegian, Measured long-range repulsive Casimir-Lifshitz forces, Nature (London) **457**, 170 (2009).

[8] R. Zhao, L. Li, S. Yang, W. Bao, Y. Xia, P. Ashby, Y. Wang, and X. Zhang, Stable Casimir equilibria and quantum trapping, Science **364**, 984 (2019).

[9] C. Henkel, K. Joulain, J.-Ph. Mulet, and J.-J. Greffet, Coupled surface polaritons and the Casimir force, Phys. Rev. A **69**, 023808 (2004).

[10] H. Iizuka and S. Fan, Casimir force between two plasmonic metallic plates from a real frequency perspective, J. Opt. Soc. Am. B **36**, 2981 (2019).

[11] M. Antezza, L. P. Pitaevskii, S. Stringari, and V. B. Svetovoy, Casimir-Lifshitz Force Out of Thermal Equilibrium and Asymptotic Nonadditivity, Phys. Rev. Lett. **97**, 223203 (2006).

[12] M. Kruger, T. Emig, and M. Kardar, Nonequilibrium Electromagnetic Fluctuations: Heat Transfer and Interactions, Phys. Rev. Lett. **106**, 210404 (2011).

[13] R. Messina and M. Antezza, Scattering-matrix approach to Casimir-Lifshitz force and heat transfer out of thermal equilibrium between arbitrary bodies, Phys. Rev. A **84**, 042102 (2011).

[14] H. Iizuka and S. Fan, Exterior tuning and switching of non-equilibrium Casimir force, J. Opt. Soc. Am. B **38**, 151 (2021).

[15] M. Kruger, G. Bimonte, T. Emig, and M. Kardar, Trace formulas for nonequilibrium Casimir interactions, heat radiation, and heat transfer for arbitrary objects, Phys. Rev. B **86**, 115423 (2012).

[16] I. Latella, P. Ben-Abdallah, S.-A. Biehs, M. Antezza, and R. Messina, Radiative heat transfer and nonequilibrium Casimir-Lifshitz force in many-body systems with planar geometry, Phys. Rev. B **95**, 205404 (2017).

[17] A. E. Rubio Lopez, P. M. Poggi, F. C. Lombardo, and V. Giannini, Landauer's formula breakdown for radiative heat transfer and nonequilibrium Casimir forces, Phys. Rev. A **97**, 042508 (2018).

[18] K. Chen and S. Fan, Nonequilibrium Casimir Force with a Nonzero Chemical Potential for Photons, Phys. Rev. Lett. **117**, 267401 (2016).

[19] G. L. Klimchitskaya, U. Mohideen, and V. M. Mostepanenko, The Casimir force between real materials: Experiment and theory, Rev. Mod. Phys. **81**, 1827 (2009).

[20] L. M. Woods, D. A. R. Dalvit, A. Tkatchenko, P. Rodriguez-Lopez, A. W. Rodriguez, and R. Podgornik, Materials perspective on Casimir and van der Waals interactions, Rev. Mod. Phys. **88**, 045003 (2016).

[21] D. A. T. Somers and J. N. Munday, Conditions for repulsive Casimir forces between identical birefringent materials, Phys. Rev. A **95**, 022509 (2017).

[22] A. W. Rodriguez, D. Woolf, A. P. McCauley, F. Capasso, J. D. Joannopoulos, and S. G. Johnson, Achieving a Strongly

Temperature-Dependent Casimir Effect, Phys. Rev. Lett. **105**, 060401 (2010).

[23] M. Dou, F. Lou, M. Bostrom, I. Brevik, and C. Persson, Casimir quantum levitation tuned by means of material properties and geometries, Phys. Rev. B **89**, 201407(R) (2014).

[24] C. Abbas, B. Guizal, and M. Antezza, Strong Thermal and Electrostatic Manipulation of the Casimir Force in Graphene Multilayers, Phys. Rev. Lett. **118**, 126101 (2017).

[25] A. W. Rodriguez, A. P. McCauley, D. Woolf, F. Capasso, J. D. Joannopoulos, and S. G. Johnson, Nontouching Nanoparticle Diclusters Bound by Repulsive and Attractive Casimir Forces, Phys. Rev. Lett. **104**, 160402 (2010).

[26] M. Levin, A. P. McCauley, A. W. Rodriguez, M. T. Homer Reid, and S. G. Johnson, Casimir Repulsion between Metallic Objects in Vacuum, Phys. Rev. Lett. **105**, 090403 (2010).

[27] A. Lambrecht and V. N. Marachevsky, Casimir Interaction of Dielectric Gratings, Phys. Rev. Lett. **101**, 160403 (2008).

[28] J. L. Garrett, D. A. T. Somers, and J. N. Munday, Measurement of the Casimir Force between Two Spheres, Phys. Rev. Lett. **120**, 040401 (2018).

[29] H. B. Chan, V. A. Aksyuk, R. N. Kleiman, D. J. Bishop, and F. Capasso, Quantum mechanical actuation of microelectromechanical systems by the Casimir force, Science **291**, 1941 (2001).

[30] L. Tang, M. Wang, C. Y. Ng, M. Nikolic, C. T. Chan, A. W. Rodriguez, and H. B. Chan, Measurement of non-monotonic Casimir forces between silicon nanostructures, Nat. Photonics **11**, 97 (2017).

[31] H. Iizuka and S. Fan, Control of non-equilibrium Casimir force, Appl. Phys. Lett. **118**, 144001 (2021).

[32] H. Iizuka and S. Fan, Trajectory tracking through the control of non-equilibrium Casimir force, J. Quant. Spectrosc. Radiat. Transfer **289**, 108281 (2022).

[33] V. S. Asadchy, M. S. Mirmoosa, A. Diaz-Rubio, S. Fan, and S. A. Tretyakov, Tutorial on electromagnetic nonreciprocity and its origins, Proc. IEEE **108**, 1684 (2020).

[34] P. Rodriguez-Lopez and A. G. Grushin, Repulsive Casimir Effect with Chern Insulators, Phys. Rev. Lett. **112**, 056804 (2014).

[35] J. H. Wilson, A. A. Allocca, and V. Galitski, Repulsive Casimir force between Weyl semimetals, Phys. Rev. B **91**, 235115 (2015).

[36] S. Fuchs, F. Lindel, R. V. Krems, G. W. Hanson, M. Antezza, and S. Y. Buhmann, Casimir-Lifshitz force for nonreciprocal media and applications to photonic topological insulators, Phys. Rev. A **96**, 062505 (2017).

[37] J.-N. Rong, L. Chen, and K. Chang, Chiral anomaly-enhanced Casimir interaction between Weyl semimetals, Chin. Phys. Lett. **38**, 084501 (2021).

[38] Z. Li and C. Khandekar, Origin of the Repulsive Casimir Force in Giant Polarization-Interconversion Materials, Phys. Rev. Appl. **16**, 044047 (2021).

[39] Q.-D. Jiang and F. Wilczek, Chiral Casimir forces: Repulsive, enhanced, tunable, Phys. Rev. B **99**, 125403 (2019).

[40] K. Fukushima, S. Imaki, and Z. Qiu, Anomalous Casimir effect in axion electrodynamics, Phys. Rev. D **100**, 045013 (2019).

[41] M. B. Farias, A. A. Zyuzin, and T. L. Schmidt, Casimir force between Weyl semimetals in a chiral medium, Phys. Rev. B **101**, 235446 (2020).

[42] D. Gelbwaser-Klimovsky, N. Graham, M. Kardar, and M. Kruger, Near Field Propulsion Forces from Nonreciprocal Media, Phys. Rev. Lett. **126**, 170401 (2021).

[43] M. G. Silveirinha, S. A. H. Gangaraj, G. W. Hanson, and M. Antezza, Fluctuation-induced forces on an atom near a photonic topological material, Phys. Rev. A **97**, 022509 (2018).

[44] J. A. Girón-Sedas, J. J. Kingsley-Smith, and F. J. Rodríguez-Fortuño, Lateral optical force on linearly polarized dipoles near a magneto-optical surface based on polarization conversion, Phys. Rev. B **100**, 075419 (2019).

[45] C. Khandekar, S. Buddhiraju, P. R. Wilkinson, J. K. Gimzewski, A. W. Rodriguez, C. Chase, and S. Fan, Nonequilibrium lateral force and torque by thermally excited nonreciprocal surface electromagnetic waves, Phys. Rev. B **104**, 245433 (2021).

[46] Y. Tsurimaki, R. Yu, and S. Fan, Moving media as photonic heat engine and pump, Phys. Rev. B **107**, 115406 (2023).

[47] L. Chen and K. Chang, Chiral-anomaly-driven Casimir-Lifshitz Torque between Weyl Semimetals, Phys. Rev. Lett. **125**, 047402 (2020).

[48] F. Lindel, G. W. Hanson, M. Antezza, and S. Y. Buhmann, Inducing and controlling rotation on small objects using photonic topological materials, Phys. Rev. B **98**, 144101 (2018).

[49] B. Strekha, S. Molesky, P. Chao, M. Kruger, and A. W. Rodriguez, Trace expressions and associated limits for nonequilibrium Casimir torque, Phys. Rev. A **106**, 042222 (2022).

[50] L. Fan, Y. Guo, G. T. Papadakis, B. Zhao, Z. Zhao, S. Buddhiraju, M. Orenstein, and S. Fan, Nonreciprocal radiative heat transfer between two planar bodies, Phys. Rev. B **101**, 085407 (2020).

[51] H. A. Haus, *Waves and Fields in Optoelectronics* (Prentice-Hall, Englewood Cliffs, NJ, 1984).

[52] There are special cases when $\tilde{F}^z_{1\to2}(\boldsymbol{k}_\parallel) = \tilde{F}^z_{1\to2}(-\boldsymbol{k}_\parallel)$. From the comparison of Eqs. (15) and Eq. (24), one can check $\tilde{F}^z_{1\to2}(\boldsymbol{k}_\parallel) = \tilde{F}^z_{1\to2}(-\boldsymbol{k}_\parallel)$ when the relation $\hat{R}_l(-\boldsymbol{k}_\parallel) = \hat{\sigma}_z\hat{R}_l(\boldsymbol{k}_\parallel)\hat{\sigma}_z$ holds. For the permittivity of Eq. (2), this relation holds when $\boldsymbol{k}_\parallel$ is parallel to the x axis, since there is no conversion between s and p polarizations. It also holds when $\boldsymbol{k}_\parallel$ is parallel to the y axis, since the permittivity $\hat{\epsilon}^S_2$ is mirror symmetric with respect to the xz plane.

[53] D. Gelbwaser-Klimovsky, N. Graham, M. Kardar, and M. Kruger, Equilibrium forces on nonreciprocal materials, Phys. Rev. B **106**, 115106 (2022).

[54] J. Zhong, K. Wang, Y. Park, V. Asadchy, C. C. Wojcik, A. Dutt, and S. Fan, Nontrivial point-gap topology and non-Hermitian skin effect in photonic crystals, Phys. Rev. B **104**, 125416 (2021).

[55] S.-A. Biehs, P. Ben-Abdallah, F. S. S. Rosa, K. Joulain, and J.-J. Greffet, Nanoscale heat flux between nanoporous materials, Opt. Express **19**, A1088 (2011).

[56] I. S. Nefedov and J. M. Rubi, Lateral-drag propulsion forces induced by anisotropy, Sci. Rep. **7**, 6155 (2017).

[57] B. Hu, Y. Zhang, and Q. J. Wang, Surface magneto plasmons and their applications in the infrared frequencies, Nanophotonics **4**, 383 (2015).